Journal of Mechanical Engineering Research and Developments
ISSN: 1024-1752
Website: http://www.jmerd.org
Vol. 39, No. 1, 2016, pp. 1-10

The Research of High Precision and Big Area Two-Dimensional Laser Controlling Reflection Platform

L. T. Xue[†‡*], X. D. Han[†], H. K. Wang[†], T. Chen[†], F. Y. Li[§] &, A. B. Zoss[††]

[†]Changchun Institute of Optics, Fine Mechanics and Physics, Chinese Academy of Sicences, Changchun l30033, China, *Email: lglwfw@163.com
[‡]University of Chinese Academy of Sciences, Beijing 100049, China
[§]Yonsei University, Seoul, Korea
[††]Mechanical Engineering department, University of California, Berkeley, CA, USA

ABSTRACT: Laser mirror optical system commonly used in the structure, mirror with two-dimensional motion function is the laser beam direction accurately control the necessary parts of the system. The collimation characteristics of laser beam is applied to the far distance interference decision must have the very high accuracy laser reflection platform two-dimensional laser at the outlet of the control, in order to ensure the accuracy of the laser spot position in the. In addition, because the laser transmission characteristics of laser jamming equipment limitations at the outlet of the need to have a certain diameter, this needs to carry on expanding beam corresponding after the laser emission to the two-dimensional control platform and the final launch out. Therefore the development of two-dimensional with large target surface high accuracy control platform is one of the key technologies in the field of laser interference. With the development of a certain type of multi wavelength laser jamming equipment as the background, using UG software design, simulation analysis and experimental study on the detection methods such as having a two-dimensional laser reflection platform closed-loop control adjustment function. The platform effective laser reflector sizes up to 100mmX100mm. By the simulation and actual test out of the way of the positioning accuracy, fixed-point test repeatability and impact vibration test on the platform, the platform measured control accuracy better than 30 rad, and the adjusting range of the two directions are more than 1mrad. The conclusion can be obtained the target with precision adjustment function of laser reflection surface of two-dimensional control platform.

KEYWORDS: Laser beam; Laser application; Photoelectric control; Platform design.

INTRODUCTION

Laser jamming system beam control system is one of the key technologies essential. Reflected light beam is commonly used beam angle control. This requires high-precision control can be realized to control the angle of the mirror. Mostly due to the interference of laser action at a distance, so near the angle control must meet a small angle to the distant high-precision control and accurate laser spot irradiated target a specific location. At the same time this control to adjust the amount of each platform in the direction of the need to reach a certain range, the only way to meet the laser jamming system at a distance, precise beam direction control within a certain area. Another current multi-system laser jamming systems are multi-band fusion [1-3]. Different bands are different laser output, and with the aim of transmitting a turntable, requiring different laser output of the laser beam combiners, and ultimately the formation parallelism and very high degree of coincidence of the laser beam. Common means of achieving this end is to use a plurality of two-dimensional adjustment of each console precise control of laser beams. One of the difficulties that currently exist in the field is due to the higher control requirements of the laser beam, tuned system installed when the experiment is successful, if there is outside interference such as oil machine vibration, load the car to move around in, and even the ambient temperature changes may have resulted in the beam deviation [4]. The real-time anti-interference ability is poor. Laser jamming system in a variety of optical components to withstand the power density of the laser is limited, and therefore the laser beam is expanded beam to the spot diameter becomes large and then reflected off by the two-dimensional adjustment stage has become commonly used in current engineering applications A method of reducing power density method, which requires a two-dimensional adjustment stage has a sufficient reflection area [5]. The current station has a lot of finished two-dimensional adjustment, such as PI produced by piezoelectric ceramic drive elements represented by two-dimensional console, these adjustments apply to photovoltaic station interference system has the advantages of quick response speed, but it also has a carrying capacity low, the area is not large enough to point directly to the precise feedback beam and other shortcomings [6-9]. Therefore, the development of a two-dimensional console to meet the requirements of the above functions has become one of the key technologies in this field must be a breakthrough [10-12]. In this paper, the development of a certain type of photovoltaic systems for background interference, explores the laser beam combining precision and laser pointing

DOI: 10.7508/jmerd.2016.01.001

accuracy plays a key role in a closed-loop real-time 2D console. First, control theory and design requirements of the system are analyzed, and then the various subsystems of the system were used to select and discussion, but according to the design requirements with UG software design of the system structure, and finally the system was appropriate simulation and experiment, the corresponding analytical results, by comparing the results obtained with the design requirements of the system reasonably valid conclusions.

TWO-DIMENSIONAL PLATFORM CONTROL THEORY AND DESIGN REQUIREMENTS

Control Principle

In the laser beam combining laser jamming system PSII way directional control over the use of the optical path pointing to the monitoring unit and two-dimensional oscillating mirror automatic closed-loop control, monitoring optical filters corresponding to each laser wavelength with automatic switching function, by laser energy attenuation measures to prevent each band laser on surveillance CCD damage. Beam combining device, for each laser with the corresponding two-dimensional swing sets corresponding bearing beam combiner lens composed of two-dimensional control oscillating mirror. Two-dimensional oscillating mirror controller to control the optical path of the laser beam output monitoring unit off target amount for angular position feedback control of two-dimensional oscillating mirror movement in two directions perpendicular to each other, automatic compensation due to the light-disorders, structural deformation, stress and deformation , ambient temperature changes, vehicle transportation and other factors offset the light path. To achieve precise control of two-dimensional laser beam, the structure, the two-dimensional control oscillating mirror selected small and thin, resistant to vibration, difficult to damage, high sensitivity and strong shear piezoelectric PZT ceramics as a drive unit to achieve a two-dimensional swing sets in motion, a single PZT drive capacity of 300 Kg. Control strategy, the two-dimensional oscillating mirror control loop control strategy using precise control of the angle of the two-dimensional oscillating mirror, the feedback element of choice is the resistance strain gages, positioning accuracy and repeatability of positioning accuracy better than 5 μrad. Principles of two-dimensional structure are shown in Figure 1 console.

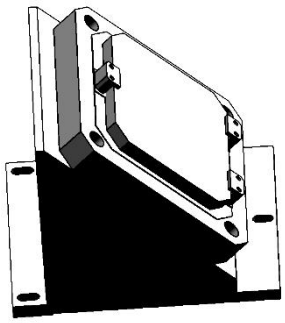

Figure 1. Two aspect console mode elements fig.

Design Requirements

The system requirements include the following aspects:

- laser beam combining superior accuracy required 30μrad;
- two-dimensional oscillating mirror precision calibration range: θx≥±1mrad;θy≥±1mrad;
- to adjust the time after beam combining belong Device Self time, with a laser-light conditions, the light beam adjustment and complete precision combined time of less than 2min;
- ray structure integrated design, structural stability, high reliability, consider sealing and dust.
- high temperature storage temperature of 60°C;
- cryogenic operating temperature of -20°C;
- vibration direction: vertical axis;
- shock wave: half sine pulse shape;
- peak acceleration: 10g.

SYSTEM DESIGN

Closed-loop monitoring console design

After closing the laser beam into the optical path of the beam expander system in setting the beam splitter, the vast majority of laser energy reflected into the main transmission system, the rest of the energy is transmitted into the post-

monitoring unit as parallel light tubes and CCD, by time-sharing monitor multiple laser spot position monitor each incident direction of laser precision dynamic control mechanism to control two-dimensional oscillating mirror for precise adjustments to ensure parallelism and four laser emitted laser pointing.

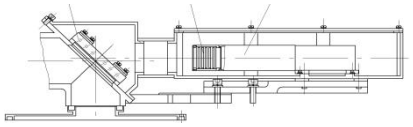

Figure 2. Light pointing and watching unit.

Monitoring unit Technical indicators are as follows: the focal length of the optical system: 1000mm; optical systems caliber: 80mm; field system: ± 300"; the incident laser divergence angle: 1.5mrad; CCD pixel size: 8μm×8μm.

Monitoring unit is using centroid tracking mode. Centroid tracking mode is selected based on image features adaptive threshold image, the image threshold binary image processing to calculate the target centroid on the binary image to the target image intensity distribution centroid tracking point, by definition, in a N×N window, its gray scale centroid position calculated by the formula 2:

$$x = \frac{\sum_{j=1}^{M} j \sum_{k=1}^{N} f(j,k)}{\sum_{k=1}^{M} \sum_{j=1}^{N} f(j,k)} \quad (1)$$

$$y = \frac{\sum_{k=1}^{N} k \sum_{j=1}^{M} f(j,k)}{\sum_{k=1}^{M} \sum_{j=1}^{N} f(j,k)} \quad (2)$$

Where: j = 1, ..., N; k = 1, ..., N; N × N window; - pixel gray value image at (j, k) point.

Because the process of calculating the centroid of the statistical averaging process, it calculates the tracking point is not the highlight of the position of the individual, but the image is a weighted average of the position of each pixel gray scale, so in order to track the centroid point, a small trace of random error high accuracy, good stability.

Dimensional adjustment console design

Beam group with close co-Beam seat, swing sets and two-dimensional beam combiner lens combined into a beam combiner mirror assembly, installation and adjustment with the positioning. The whole group together Beam fixed installations follow the principles of three-point support position, can be reduced due to the base surface deformation caused by beam pointing deviation. The design of the two-dimensional control oscillating mirror dimensions as shown.

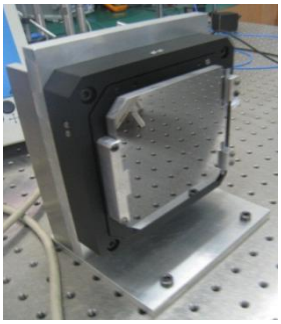

Figure 3. The practicality of mirror and reglector.

DIMENSIONAL CONSOLE TEST

Control precision repeatability test

One of the keys to the success of the two-dimensional console design is repeated in different environments positioning accuracy meets the requirements. So this paper after completing a two-dimensional console prototype design before and after environmental tests were carried out to test the positioning accuracy of the test. The test console two axes respectively tested. Figure 4 shows the same time, test method, the two-dimensional control of swing sets and other equipment Autocollimator flotation installed on the same platform, the control angle in both directions of the angle of

swing sets actual detection of the console, both were compared to a corresponding test results. Two-dimensional swing sets repeatability test site shown in Figure 4.

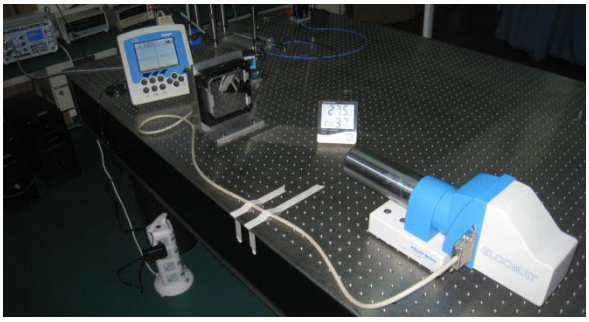

Figure 4. Console repeat precision test pattern.

The test results are listed below in chart form.

Firstly that the X-axis uniaxial test.

Positive X axis uniaxial test: Test Range: 0 "~ 200"; Test Method: Reciprocating measured 5 times along the X-axis, Y-axis unchanged. Positive X axis uniaxial test results are shown in 0, known from the test results, when the X-axis measurement to drive back and forth, and return the error is inconsistent, to process error is small, 0 "to 150" stroke within the error mean -0.10 ", the maximum error of -1.49 "; return error when compared to the larger process, 0" to 150 "in the itinerary, the mean error of 1.38" maximum error of 2.55. "

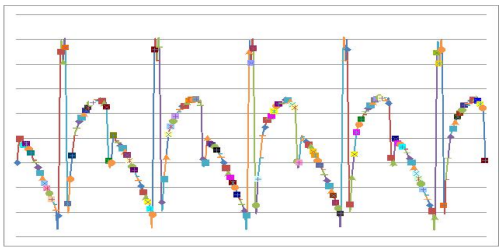

Figure 5. X axes correctitude axes test result.

X-axis negative uniaxial axle Test: Test Range: 0 "~ -200"; Test Method: Reciprocating measured 5 times along the X-axis, Y-axis unchanged. X-axis negative axle uniaxial test results shown as 0, it can be seen from the figure the better the test results of the X-axis, in a substantially error "within. Error Mean -0.69", the maximum error of 1.15. "

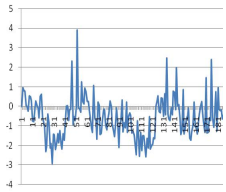

Figure 6. X axes bear axes test result.

Then the Y-axis uniaxial was tested.

Y-axis positive uniaxial axle Test: Test Range: 0"~180"; Test Method: Reciprocating measured 5 times along the Y axis, X axis unchanged. Y-axis positive axle uniaxial test results shown as 0, it can be seen from the figure the better the test results of the Y-axis, in a substantially. As shown in Figure 7 the mean error -0.54" 0"to 150"within a maximum error of 1.95 stroke.

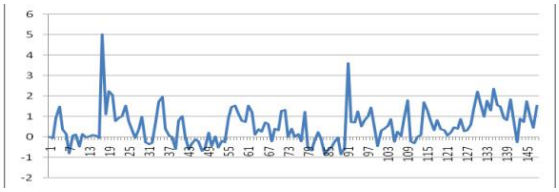

Figure 7. Y axes correctitude axes test result.

Y axis negative axle uniaxial tests: Test Range: 0 “to -200”; Test Method: Reciprocating measuring five times along the Y-axis, X-axis unchanged. Y-axis negative uniaxial test results as 0 axle shown. From the test results known, 0 “to -150” itinerary error is small, mean -0.64, maximum 2.91 “, known from experimental data analysis, measurement and forth when the Y-axis, inconsistencies go away and return error characteristics, to process the error less than the return, when to drive 0 “to -150” within the itinerary, the basic error of less than one. “

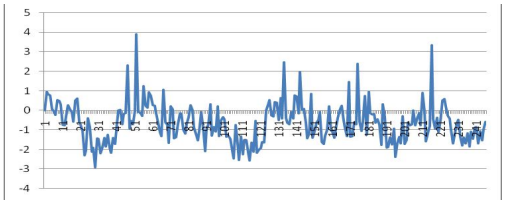

Figure 8. Y axes bear axes test result.

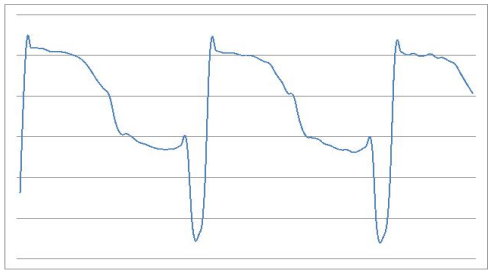

Figure 9. The X axes error curve in first quadrant.

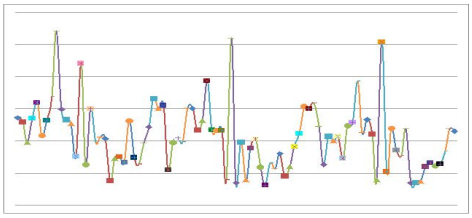

Figure 10. The Y axes error curve in first quadrant.

The second quadrant of the test range is: X: 0”~ -150”; Y: 0”~ 150”. Test Method for reciprocating along a second quadrant diagonally measured three times. In the second quadrant of the X-axis error curve shown as 0, Y-axis error curve as shown in 0. From the experimental data known, X-axis error increases with the increase of the angle setting value, 150 “near the maximum value 1.4.” Y-axis with the angle error also increases the set value, at 150 “near the maximum -4.94”, Y-axis the average error is larger than the X-axis

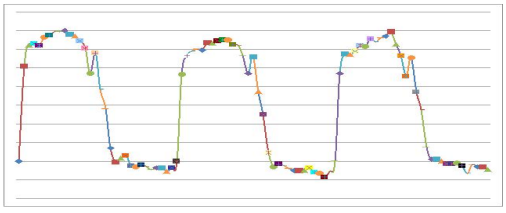

Figure 11. The X axes error curve in second quadrant.

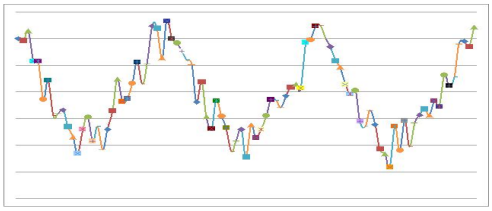

Figure 12. The Y axes error curve in second quadrant.

Third quadrant test ranges: X: 0 "~ -150"; Y: 0 "~ -150". Test methods for reciprocating along three quadrants diagonally measured three times. In the third quadrant of the X-axis error curve shown as 0, Y-axis error curve as shown in 0. From the experimental data known, X-axis error increases with the increase of the angle setting value, 150 "near the maximum value 1.39." Y-axis with the angle error also increases the set value, at 150 "near the maximum 2.41", Y-axis the average error is larger than the X-axis and Y-axis error and return to process error characteristics inconsistent, return error is larger, go away within 0 "to 130" stroke, the error is less than 1 ", return the 130" ~ 0 "in the error is greater than a stroke."

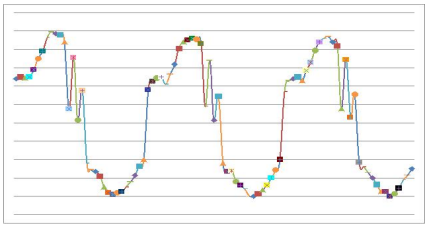

Figure 13. The X axes error curve in third quadrant.

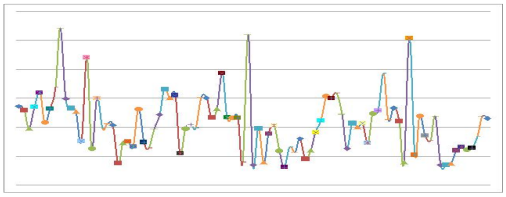

Figure 14. The Y axes error curve in third quadrant.

Fourth quadrant measurement range of X: 0 "~ 150"; Y: 0 "~ -150". Test Method for Reciprocating measured three times in the first quadrant diagonal. Test results for the fourth quadrant of the X-axis error curve as shown in 0, Y-axis error curve as shown in 0. FIG 15,16, X-axis error increases with the increase of the angle set value, at 150 "near the maximum value -4.62" and the Y axis error and return to process error characteristics inconsistent, to process error is large, to process at 130 "~ 0" stroke error is greater than a "return in 130" ~ 0 "in the itinerary, the error is less than 1." Y-axis with the angle error also increases the set value, at 150 "near the maximum 4.5."

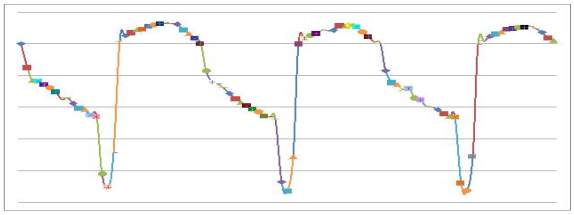

Figure 15. The X axes error curve in fourth quadrant.

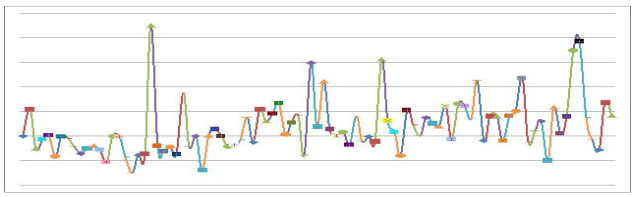

Figure 16. The Y axes error curve in fourth quadrant.

Control precision repeatability test

The quality of environmental adaptability of the two-dimensional console directly related to the optical jamming system stability. So it is necessary for environmental adaptability of the system for verification. In this paper, a method for the verification of its sine sweep vibration, the frequency range 16 ~ 200Hz, vibration acceleration of 1.5g, in three directions mutually perpendicular vibration test, a scan time of 12min, 3 cycles. Vibration test site is shown in Figure 17.

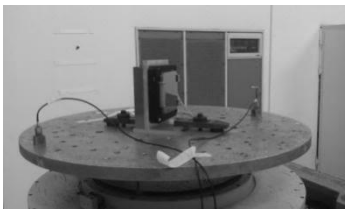

Figure 17. Two axes mirror libration test.

Semi-sinusoidal pulse impact test, the peak acceleration of 150m / s2, pulse width 11ms, the impact of the number of two mutually perpendicular directions of impact three times. Experimental results show that the two-dimensional swing sets in the large impact structures intact, which shows its good impact resistance.

X-axis uniaxial test method comprising: measuring range: 0 "~ 150"; Test Method: Five measurements reciprocating along the X axis, Y axis unchanged. Error characteristics to process and return the X axis reciprocating inconsistent measurements from the test results to know, backhaul error is small, 130 "~ 0" stroke within the error is less than 1 ", to process larger error, the error is greater than one."

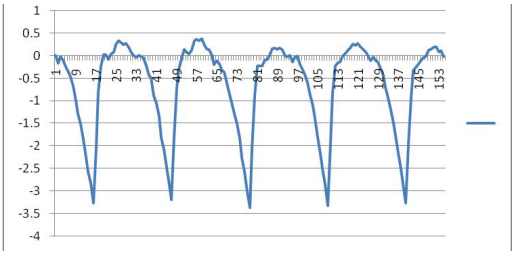

Figure 18. X axes correctitude axes test result.

X-axis negative uniaxial axle test range: 0 "-150"; Test Method: Reciprocating measured 5 times along the X-axis, Y-axis unchanged. X-axis negative axle uniaxial test results shown as 0, it can be seen from the figure the better the test results of the X-axis, in a substantially error "within. Error Mean -0.22", the maximum error of 1.04. "

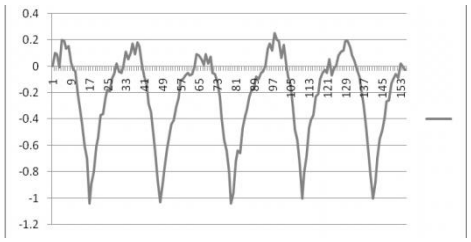

Figure 19. X axes bear axes test result.

On the Y-axis uniaxial test results in the range 0 'to 150'; Test Method: Reciprocating measured 5 times along the Y axis, X axis unchanged. Y-axis positive axle uniaxial test results shown as 0, it can be seen from the figure the better the test results of the Y-axis, the basic error in a "near changes, the mean error of -0.30."

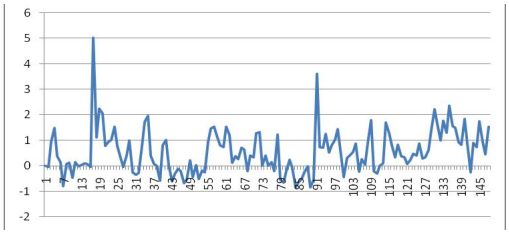

Figure 20. Y axes correctitude axes test result.

Y-axis negative axle uniaxial test range: 0" to -150"; Test Method: Reciprocating measuring five times along the Y-axis, X-axis unchanged. Y-axis negative uniaxial test results as 0 axle shown. Know from the test results, the mean error 0.56 "maximum error 3.84."

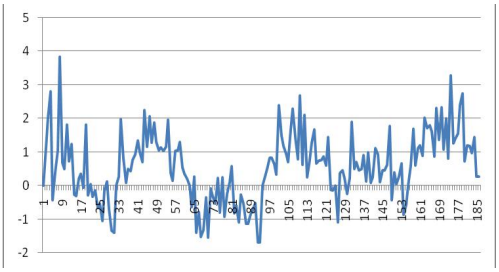

Figure 21. Y axes bear axes test result.

Test range of the first quadrant as: X: 0 "~ 150"; Y: 0 "~ 150". Test Method for Reciprocating measured three times in the first quadrant diagonal. X-axis in the first quadrant error curve is as shown 0, Y-axis error curve as shown in 0. Known from experimental data, X-axis to drive at 0 "to 130" stroke within the basic error in a "less than, 150" at the maximum error of 3.16 ", the return journey to the X-axis error compared with larger .Y axis error angle setting value increases, in the 150 "near the maximum value 25.22."

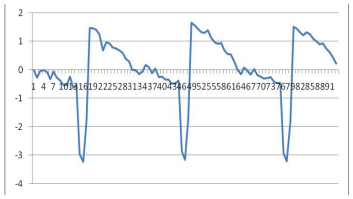

Figure 22. The X axes error curve in first quadrant.

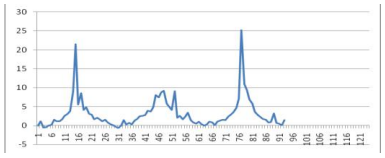

Figure 23. The Y axes error curve in first quadrant.

The second quadrant test ranges: X: 0 "~ -150"; Y: 0 "~ 150". Test Method for reciprocating along a second quadrant diagonally measured three times. In the second quadrant of the X-axis error curve shown as 0, Y-axis error curve as shown in 0. Known from the experimental data, X-axis in a substantially "within .Y axis error increases with the increase of the angle setting value, 150" near the maximum -4.96 ", Y-axis the average error is larger than the X-axis.

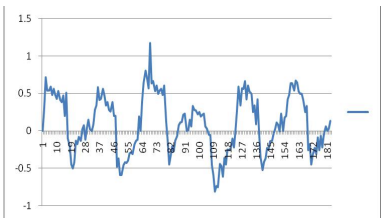

Figure 24. The X axes error curve in second quadrant.

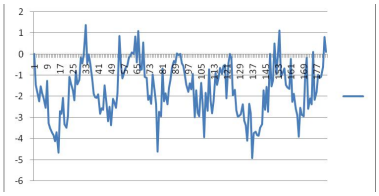

Figure 25. The Y axes error curve in second quadrant.

The third quadrant of the test range: X: 0 "~ -150"; Y: 0 "~ -150". Test Method for reciprocating along a third quadrant diagonally measured three times. In the third quadrant of the X-axis error curve shown as 0, Y-axis error curve as shown in 0. Known from experimental data, X-axis error is basically in a "less than, the maximum error of 1.02." X axis Y axis error compared to the larger, after removing the outliers, the maximum error is 3.11. "

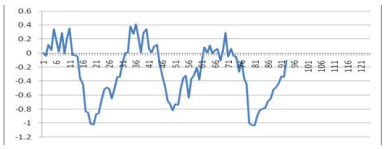

Figure 26. The X axes error curve in third quadrant.

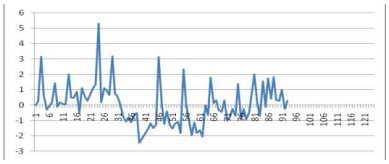

Figure 27. The Y axes error curve in third quadrant.

Measuring range of the fourth quadrant: X: 0 "~ 150"; Y: 0 "~ -150". Test methods for reciprocating along the diagonal measurement of the fourth quadrant 5 times. The fourth quadrant of the X-axis error curve shown as 0, Y-axis error curve as shown in 0. From the experimental data known, X-axis error increases with the increase of the angle setting value, 150 "near the maximum value -4.63." Y axis error is large compared to the X-axis, the maximum error of 8.53. "

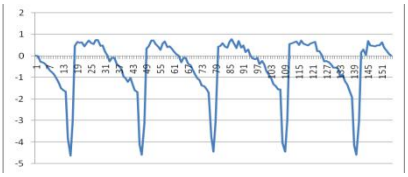

Figure 28. The X axes error curve in forth quadrant.

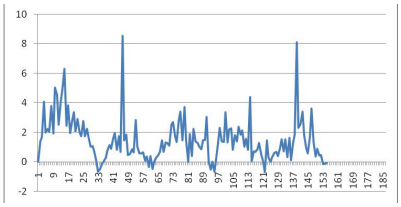

Figure 29. The Y axes error curve in forth quadrant.

See comparison of the position of the origin 0 before environmental testing. As can be seen from the table before and after environmental testing home position deviation is not, it is possible to reset the precision and bias-related position (using visual light tube and glue in place pedestal seat 502 small mirror self registration method to achieve position reset cross returned as vague, targeting difficult)

Table 1. The origin position warp between before and after of the condition test.

set	X(″)	Y(″)
Environmental testing before	11	0
After environmental testing	28.32	15.84

Repeat two-dimensional swing sets down power position changes as shown in Table 1. Swing sets before and after the two-dimensional X-axis is repeated up and down the average change in the amount of electricity 0.28 ", the amount of the average change in the Y-axis 0.12", a small amount of change.

Test Analysis

For two-dimensional control before and after environmental testing oscillating mirror positioning accuracy tests were carried out, pointing repeatability and reproducibility of the upper and lower electrical test, and the test data were compared, results showed that the two-dimensional oscillating mirror control with good reproducibility.

Two-dimensional swing sets before and after environmental testing performance comparison below. X-axis and Y-axis uniaxial test results before and after the environmental test is not very different; quadrant test results before and after the vibration difference differ, but the X-axis error characteristics remain basically unchanged at 0 “C to 130” within the error of the stroke is substantially smaller than 1 “, Y axis error becomes large .X axis error is small compared to Y axis error. uniaxial test, when the X-axis measurement accuracy in a small angular range (0 “to 150”), the error is substantially less than 1. “Y-axis uniaxial measurement error is large, more than one. “When the four-quadrant test, inconsistent error characteristics of each quadrant, the third quadrant preferably .Y axis X axis error compared to the actual measured value larger .X linear axis and Y-axis are both excellent. the actual measurement data of an experiment in which, for example, 0 and 0 respectively X-axis and the setpoint measured values and the Y-axis in FIG comparing setpoint and measured value comparing FIGURE As can be seen from the figure, the actual measured values and the Y-axis actual measured value and set value X axis basically consistent, good linearity. two-dimensional position of the origin swing sets little change before and after environmental testing.

ACKNOWLEDGMENT

This paper explored the principles of two-dimensional console feedback using a new method of real-time adjustment, this method can solve the problems of the current system of environmental adaptability restrict the development of such devices. For the development of this type of equipment is important. In this paper, a high-precision laser for laser interference device dimensional console bundle together a prototype design. And its overall accuracy test was also carried out to test and analyze its environmental adaptability. Through the analysis of the test results obtained in this system can meet the system requirements for accuracy specification conclusion.

REFERENCES

[1] M.R. Suite, H.R. Burris, C.I. Moore, et al., “Fast steering mirror implementation for reduction of focal-spot wander in a long-distance free-space communication link,” Proc. of SPIE, 2004, Vol. 5160:439-446.

[2] ZHANG L M, GUO J, “Simulative research on dual X-Y axis control of fast steering mirror,” Optics and Precision Engineering, 2005(13):142-147. (in Chinese)

[3] Felix E. Morgan, Steven R. Wasson a, Jamison J. London, et al., “Large, high performance, fast steering mirrors with FPGA-embedded controls,” Proc. of SPIE, 2009, Vol. 7466:74660H1-74660H10.

[4] LING N, CHEN D H, GUAN CH L, et al., “Two-dimension piezoelectrical fast steering mirror,” Opto-Electric Enginnering, 1995, 22(1):51-60. (in Chinese)

[5] Francisc M. Tapos, Derek J. Edinger, Timothy R. Hilby, et al., “High bandwidth fast steering mirror,” SPIE, 2005, Vol. 587707:01-14.

[6] SHAO S, GAO Y G, GUO J, et al., “Design of two-dimensional fast-steering cooling mirror equipment,” Optics and Precision Engineering, 2009, 17(3):493-498. (in Chinese)

[7] Michael Sweeney, Gerald Rynkowski, Mehrdad Ketabchi, et al.. Design Considerations for Fast Steering Mirrors (FSMs). SPIE, 2002, Vol. 4773:63-73.

[8] ZHANG L M, GUO J, CHEN J, “Summary of the mechanic structure for fast-steering mirrors,” Ome Informtion, 2005(3):21-24. (in Chinese)

[9] QIU X B, DOU L H, SHAN D SH, et al.. Design of active disturbance rejection controller for electro-optical tracking servo system. Optics and Precision Engineering, 2010, 18(1):220-226. (in Chinese)

[10] TANG T, HUANG Y M, FU CH Y, et al., “Acceleration feedback of a CCD-based tracking loop for fast steering mirror ,” Optical Engineering, 2009, 48(1): 013001

[11] WANG Y F, “Computer Aided Engineering Analysis and Calculation of the Light Weight Primary Mirror ,” Optics and Precision Engineering, 1995, 3(6):66-70. (in Chinese)

[12] Paul R.Yoder, Jr, “Opto-Mechanical Systems Design,” China Machine Press, 2006.